

# From ISAAC to GOLIATH, or better not!? Infrared Instrumentation Concepts for 100m Class Telescopes

Hans Ulrich Käuffl & Guy Monnet  
European Southern Observatory

## ABSTRACT

A projection of the future of infrared instrumentation is given using the evolution of infrared K-band spectroscopy at ESO as an example. The limitations for a future increase in sensitivity, resulting from instrument improvements alone, for a given telescope size are outlined. Based on the experience with the present ESO Infrared Instruments (ISAAC, CONICA, VISIR and CRIRES) concepts for instrumentation covering the wavelength range from 1-25 $\mu$ m micron are presented. In all cases adaptive optics is considered as an integral part of the instruments. The requirements for the adaptive optics systems will be given differentiated for each instrument case. Performance figures for the most promising instrument and adaptive optics concepts will be estimated, based on an extrapolation of today's technologies. The performance potential of an 100m class telescope will be compared to space missions with cryogenic telescopes (ISO, SIRTf and the NGST). Starting from today's astronomical results with the LaSilla telescopes some selected potential scientific highlights for far-infrared astronomy are sketched.

## INTRODUCTION: The History of K-Band Spectroscopy at ESO

ESO has recently commissioned two new general purpose common user instruments for the near-infrared: SOFI at the 3.5m NTT on La Silla and ISAAC on Paranal at the VLT Unit Telescope #1 (Antu) (see e.g. Moorwood et al. 1998, 1999). These two instruments are the culmination of 20 years of infrared instrumentation development at ESO. In table 1 we summarize the technical progress, by sketching the evolution of K-band spectroscopy at 3.5m class telescopes at ESO as a representative example.

Telescope	Year	Instrument	Detector	$\frac{\lambda}{\Delta\lambda}$	Sensitivity $1\sigma, 60s$
3.6m	1980	Photometer f/8 (CVF)	1 pix InSb	50	$\approx 6 \times 10^{-16} \frac{W}{m^2}$
3.6m	1984	Photometer f/35 (CVF)	1 pix InSb	50	$\approx 3 \times 10^{-16} \frac{W}{m^2}$
3.6m	1986	IRSPEC (grating)	32 pix InSb	2000	$\approx 3 \times 10^{-17} \frac{W}{m^2}$
3.5m NTT	1991	IRSPEC (grating)	58 $\times$ 62 pix InSb	3000	$\approx 7 \times 10^{-19} \frac{W}{m^2}$
3.5m NTT	1998	SOFI (grism)	1024 <sup>2</sup> pix HgCdTe	2000	$\approx 5 \times 10^{-20} \frac{W}{m^2}$

**TABLE 1:** Sensitivity Versus Time: K-band Spectroscopy at ESO

From table 1 it is evident that:

- the sensitivity for emission line objects has improved 4 orders of magnitude in 20 years (i.e. the 1980 photometer as compared to SOFI used less than the size of a coin of the collecting area of the 3.6m!)
- in parallel to the sensitivity gain an effective 4 arcmin slit length was added

Moreover source acquisition has been facilitated tremendously while operations now are literally free of overhead. In addition users of SOFI today enjoy the multiplex advantage of a 1024<sup>2</sup> detector compared to a single-channel photometer in 1980. To assess the prospects of astronomical research in the future the following question needs to be analyzed: *To which extent will the historic trend of an average gain in sensitivity of 0.5<sup>mag</sup>/year persist?* Looking at SOFI at ESO's NTT provides for an answer. From table 2 which summarizes important characteristics it is obvious that the room for future improvements is very restricted:

detector size:	1024 <sup>2</sup>
field of view:	300 x 300 <i>arcsec</i> <sup>2</sup> (seeing Nyquist sampled) or 75 x 75 <i>arcsec</i> <sup>2</sup> (Airy pattern Nyquist sampled)
detector:	quantum efficiency: 65% Read-Out Noise 2-10e <sup>-</sup> dark current negligible
instrument efficiency:	25-50% (depending on mode)

**TABLE 2:** Technical Characteristica of SOFI

- next generation detectors are basically *only* larger (for a status report on detector development work at ESO see e.g. Finger et al, 1998)
- telescope mirror coatings could be improved (Gold or protected Silver rather than Aluminum)
- better grisms (e.g. cross dispersed Echelle mode, Käuffl et al., 1998)

In conclusion, apart from field size and the implementation of new modes such as multi-object or integral field capabilities, the maximum improvement to be anticipated for a hypothetical SOFI successor could be at best a factor of 2. SOFI is a representative example for the entire IR; a similar situation exists for ISAAC at the VLT ( $1\mu m \leq \lambda \leq 5.2\mu m$ ) and soon for TIMMI2 at 3.6m ( $7.7\mu m \leq \lambda \leq 24\mu m$ ; c.f. Reimann et al. 1998).

A substantial gain in sensitivity for ground-based infrared instrumentation w.r.t. today's state-of-the-art instrumentation thus can only be achieved via an increase in collecting area, i.e. it needs a considerably larger telescope. Before jumping to conclusions, however, the question whether an extremely large telescope is really the next logical step for ground-based IR astronomy, deserves further analysis. Specifically one has to assess in detail:

- What are the fundamental limitations of ground based IR astronomy? This requires to analyze in detail: signal to noise ratio, image quality, atmospheric seeing and potential of adaptive optics, potential instrument designs/bottlenecks.
- How competitive is ground based astronomy in the IR compared to space based platforms?
- Is there a convincing science case?

We will try to approach an answer to these points by drawing up a strawman instrumentation plan which can then be compared to the scientific requirements.

## SENSITIVITIES AND THE COMPARISON TO SPACE

The following discussion will be restricted to detection limits for unresolved point-like sources.<sup>1</sup> We will refer to 100m-class telescopes by the ESO preferred acronym OWL (Overwhelmingly Large Telescope, see the corresponding ESO contributions in these proceedings). In table 3 infrared instrumentation performances for OWL are compared to an ideal photon counting system in space (assumptions for the ideal case: read-noise 0e<sup>-</sup>, total system efficiency 100%, dark-current 0e<sup>-</sup>/s, telescope thermal emission and other sources of background irradiation negligible). We assume as the only source of noise for the ideal photon counter the shotnoise of the source signal with Gaussian distribution. We have chosen to compare OWL versus an ideal receiver, because as of today there is not sufficient technical information to compare the Next Generation Space Telescope (NGST) in full detail to groundbased astronomy. It is obvious, however, that NGST can hardly achieve the performances given in table 3. Any realistic system will be hampered at least by zodiacal light, stray light, a non-negligible telescope temperature, cosmic rays, persistence effects, read-out noise, detector dark current and it will have at best 70% efficiency. In table 3 we give a raw estimate of the degradation which tends to increase dramatically towards longer wavelengths because of telescope temperature, zodiacal emission and stray light resulting from thermal radiation of the NGST sun-shield.

<sup>1</sup>This favours groundbased astronomy slightly but puts stringent requirements on the telescope optics and the adaptive optics system.

atm. Band $\lambda[\mu m]$	J	H	$K_s$	L	N	Q
	1.25	1.6	2.1	3.5	10	20
ideal 8m dia. receiver $1.22\frac{\lambda}{D}$	$31.6^{mag}$ 39mas	$31.2^{mag}$ 50mas	$30.6^{mag}$ 66mas	$29.8^{mag}$ 110mas	$27.6^{mag}$ 315mas	$26.1^{mag}$ 629mas
real receiver degradation (see text)	$1.0^{mag}$	$1.3^{mag}$	$1.7^{mag}$	$2.0^{mag}$	$3.0^{mag}$	$6.0^{mag}$
OWL $\sigma_{psf}$	$30.5^{mag}$ 30mas	$30.0^{mag}$ 20mas	$29.7^{mag}$ 10mas	$26.1^{mag}$ 10mas	$19.5^{mag}$ 25.2mas	$16.1^{mag}$ 50.3mas
OWL++ $\sigma_{psf} = 1.22\frac{\lambda}{D}$	$33.0^{mag}$ 3.1mas	$31.7^{mag}$ 4.0mas	$30.4^{mag}$ 5.5mas	$26.1^{mag}$ 8.8mas	$19.5^{mag}$ 25.2mas	$16.1^{mag}$ 50.3mas

**TABLE 3:** Comparison of Sensitivity Limits

educated guess for OWL and an ideal 8m diameter photon-counter; limiting magnitudes for a spatially unresolved source  
note: • OWL++ stands for full adaptive optics correction, OWL for partial correction in the near IR

- the NGST (Next Generation Space Telescope will typically fall short by a factor of 10 (see text) from an ideal receiver.
- Assumptions: J, H, and  $K_s$  performances are based on ISAAC/VLT results; for  $\lambda \geq 3\mu m$ : OWL temperature 283K, OWL emissivity 0.85, temperature of atmospheric absorption layers 253 K; det. q.e.  $\eta = 0.7$ ; efficiency of cold optics: 0.7; atmospheric emissivity 0.15 (0.5 at  $20\mu m$ )  $\frac{\lambda}{\Delta\lambda} = 10$  and  $\frac{\lambda}{N} = 10$  in 3600s

As can be seen from table 3, up to  $\lambda \approx 4\mu m$  infrared instrumentation at OWL - within the general limitations of ground based astronomy working through a comb of sometimes inconveniently placed absorption lines - always is competitive or superior to an 8m space telescope while featuring up to an order of magnitude better spatial resolution, provided adaptive optics is available (see below). In the classical thermal infrared a space based platform has a sensitivity advantage but typically only by factors of 10-100. For many scientific applications, however, spatial resolution will be more important than the ultimate sensitivity. It should be noted here that for high resolution spectroscopy the balance of sensitivity will be shifted substantially towards OWL.

## DAVID versus GOLIATH: Dedicated Active Optics Integrated Designs

It is well established that all parameters relevant for seeing and seeing-corrections via adaptive optics (AO) are a function of wavelength. Table 4 summarizes these parameters as a function of wavelength following the *conventional wisdom* of adaptive optics (c.f. R. Wilson 1999 and references therein). Moreover we ignore the concepts of multi-conjugate plane adaptive optics (c.f. Rigaut, Ragazzoni et al., or Hubin & Le Louarn, these proceedings)<sup>2</sup>.

$\lambda [\mu m]$ standard designation	0.5	1.0	1.3	1.6	2.0	3.5	10	20
			J	H	$K_s$	L	N	Q
$r_0 [m]$	0.20	0.46	0.63	0.81	1.06	2.07	7.28	16.7
$\Phi_{isop} ["]$	3.5	8.00	11.0	14.1	18.5	36.2	127.4	292.8
$t_{coh} [ms]$	10	23	31.5	40.4	53	103	364	838

**TABLE 4:** Basic Adaptive Optics Parameters for OWL in the IR ( $r_0$  is Fried's parameter,  $\Phi_{isop}$  is the size of the isoplanatic patch and  $t_{coh}$  the atmospheric coherence time.

Table 4 illustrates the well known fact, that the requirements for an adaptive optics system rapidly relax when the operating wavelength increases (after all the complexity of an adaptive optics system scales to first order with  $(r_0 \times t_{coh})^{-1}$  while the size of the isoplanatic patch approaches values which allow for reasonable field-of-views without the need for a multiple conjugate plane AO system. In table 5 we summarize the most important technical design parameters for an infrared adaptive optics system at OWL.

<sup>2</sup>In most cases a larger field of view than the *normal* isoplanatic patch can not easily be accommodated in instrumentation. Still in the near-infrared the concepts need further attention as the increase in Strehl ratio may not be negligible.

$\lambda$ [ $\mu\text{m}$ ] standard designation	1.3 J	1.6 H	2.0 $K_s$	3.5 L	10 N	20 Q
$n_{\text{actuators}}$	$10^5$	$6 \cdot 10^4$	$3.5 \cdot 10^4$	9300	755	143
$\text{bandwidth}[\text{Hz}]$	63	50	38	19	5.5	2.4
$\text{Ø}_{\text{activemirror}}$ [mm]	635	494	377	193	352	814
sky-cov $_{G-Equ}$ [%]	TO	TO	0.2	30	100	100
sky-cov $_{G-Pole}$ [%]	TO	TO	0.6	100	100	100
guide-star band	H, K	J, K	J, H	J, H, K	J, H, K	J, H, K
$T_{0.05}$ [K]	261	257	250	235	180	145
max. flexure [ $\mu\text{m}$ ]	0.13	0.16	0.20	0.36	1.02	2.03

**TABLE 5:** Resulting Technical Requirements for an Adaptive Optics System for OWL in the IR. The diameter of the adaptive optics active correction mirror is derived either from the assumption that the minimum spacing between two adjacent actuators should not exceed 2 mm or that the maximum off-axis angles of the optical path in this plane should not exceed  $\pm 5^\circ$ .  $T_{0.05}$  is the maximum operation temperature where the thermal background emission of the adaptive optics system can be ignored. The sky coverage, differentiated for the galactic pole and equator for natural guide-star operation is taken from Merkle 1988 and most likely conservative; TO here means, that only few adaptive optics *Targets of Opportunity* can be observed. The flexure requirements are illustrated by giving the tolerance for the maximum movement which can be allowed between the AO tip-tilt sensor and the infrared science array, projected into the OWL focal plane<sup>3</sup>.

Table 5 shows that the AO requirements are extremely different for different  $\lambda$ s and a *one-size-fits-all* approach to adaptive optics in the infrared is problematic. At this point please be reminded of the title of this paper: *From ISAAC to GOLIATH, or better not!?*. Extrapolating from the experience with ISAAC<sup>4</sup> at the VLT, an 8m telescope, to a similar concept for OWL leads to a truly BIG instrument, hence the acronym GOLIATH seems appropriate. While not yet knowing exactly, what GOLIATH ultimately may stand for, GOLIATH may be the easy victim of DAVID the Dedicated Active Optics Integrated Design. The cooling requirements for IR AO are complementary to the complexity. Correspondingly the flexure requirements can be relatively relaxed, the longer the wavelength. While the *flexure requirements* in table 5 give only the order of magnitude of stiffness to be achieved, it is obvious that they can be much easier met, if the AO system and the scientific instrument are integrated into the same optical structure, i.e. if they are part of one cryomechanical assembly. For any IR instrument this concept automatically lends itself to a cryogenic AO system and to an infrared wavefront sensor. Detector technology for suitable IR-AO sensors, different from those systems used for scientific purposes, featuring almost perfect performance exists (see e.g. Kozłowski et al., 1996). Moreover, using the near IR (J, H, K) for image analysis has at least three distinct advantages: the correction for differential atmospheric refraction is considerably facilitated, anonymous field stars tend to be red and chopping<sup>5</sup>, e.g. by load switching, can be integrated in the AO train. A slight disadvantage of the DAVID concept is, that a field approaching the maximum isoplanatic area needs to be transferred through the entire cryogenic adaptive optics train to achieve the optimum sky coverage with natural guide stars.

## AN OWL STRAWMAN INFRARED INSTRUMENTATION PLAN

What would a DAVID look like? Nearly all ESO instruments follow the EFOSC<sup>6</sup> approach, i.e. they are focal reducers consisting of an accessible focal plane, a collimator, an accessible pupil plane and a camera, normally with variable magnification. Grisms are generally being used as dispersive elements. In the focal plane slits, slitmasks, fibre bundles or other assemblies allowing for multi-object or integral field spectroscopy can be positioned. This generic principle is being applied in the wavelength range from  $\approx 350\text{nm} - 24\mu\text{m}$ . So it seems the obvious choice for

<sup>3</sup>The OWL f# is assumed to be 6 and an image blur equivalent to  $0.6 \frac{\lambda}{D}$  is tolerated.

<sup>4</sup>ISAAC stands for Infrared Spectrometer and Array Camera

<sup>5</sup>As the secondary mirror of OWL will have 30m diameter M2-chopping is most likely impossible.

<sup>6</sup>EFOSC2 ESO Faint Object Spectrograph and Camera is one of ESO's workhorses at the 3.6m telescope, LaSilla

and OWL-DAVID, but also for an OWL GOLIATH (i.e. an instrument not using active optics).

#	Instrument Type	$\lambda$ -range [ $\mu m$ ]	size estimate [m]	detector	field $\square''$	main technical risk areas	pupil dia. [mm]	comp. sensitivity	to space image quality	hitch-hiker
1	GOLIATH no AO	<u>1-2.5</u>	$\emptyset 10 \times 3$	$4K \times 4K$ HgCdTe	$60 \times 60$ or $120 \times 120$	size, flexure filters	160 320	-- -	- -	yes
2	IR-EFOSC OWL AO	<u>1-2.5</u>	$\emptyset 2 \times 2$	$8K \times 8K$ HgCdTe	$20 \times 20$	flexure atm. disp.	50	-	++	no
3	NGS-DAVID +IR-EFOSC	<u>1-2.5</u>	$\emptyset 3 \times 3$	$8K \times 8K$ HgCdTe	$20 \times 20$	size, flex. AO-mirror 35000 act., 40Hz	50	+ restr. cover	++ sky age	no
4	NGS-DAVID +IR-EFOSC	<u>3.5-5.2</u>	$\emptyset 5 \times 4$	$8K \times 8K$ InSb	$40 \times 40$	size, flex. optics, data	110	o	++	yes
5	NGS-DAVID +IR-EFOSC	<u>7.7-24</u>	$\emptyset 5 \times 4$	$8K \times 8K$ ????	$120 \times 120$	size, flex. optics, data	330	-	++	yes
6	NGS-DAVID +hi-res-spectr. $\frac{\lambda}{\Delta\lambda} \approx 5 \cdot 10^5$	<u>1.1-5.2</u>	$\emptyset 5 \times 6$	$4K \times 12K$ InSb	n.a.	AO, size, optics, flex.	500	n.a.	n.a.	no
7	NGS-DAVID +hi-res-spectr. $\frac{\lambda}{\Delta\lambda} \approx 3 \cdot 10^5$	<u>7.7-14.0</u>	$\emptyset 5 \times 6$	$4K \times 12K$ ????	n.a.	size, optics, flex.	500	n.a.	n.a.	no

**TABLE 6:** The OWL Strawman Infrared Instrumentation Plan (very condensed version). It lists very schematically 7 basic instruments. The column  $\lambda$ -range gives the operating wavelength for each instrument whereby, if appropriate, the optimized operation wavelength is underlined. The size estimates are always based on the approximate size requirements of the collimators (instruments #1&2 have only the *normal EFOSC* collimator, instruments #3&4 need in addition 2 more collimators or Offner type or other relays to position the adaptive mirror and the tip-tilt mirror, for instrument #5 it is assumed that no particular tip-tilt stage is required; for the spectrographs (instruments #6&7) it is assumed that a  $\approx 2m$  long Echelle grating is being illuminated by a 500mm  $\emptyset$  collimated beam. The detector sizes are based on Nyquist sampling of the OWL diffraction pattern in the field, for instruments #2-#5 which use AO. The spectrograph detectors are based on Nyquist sampling of a diffraction limited slit, whereby the format allows with cross-dispersion to cover typically 10% of the spectrum. Without cross-dispersion any implementation of integral field spectroscopy with typically  $50 \times 50$  pixels is conceivable. The maximum pupil diameters have been estimated under the assumption that off-axis beams in the optical train should not exceed  $\pm 5^\circ$  (both to ease the optics design and to allow for the use of narrow-band filters). The last row indicates whether the instrument could be usefully employed in hitch-hiker mode.

The instrumentation plan presented in table 6 is a first educated guess of what instruments are required to exploit the unique capabilities of an OWL (spatial resolution, collecting area and hitch-hiker capabilities). Especially the instruments #1 and #2 need a very intense analysis of the scientific merits. For #1 there may be excellent areas of research if the collecting power of OWL but not the full spatial resolution in combination with field are required (e.g. the ODF, the QWL Deep Field). Instrument #2 - using the facility AO system - will have a strongly compromised sensitivity w.r.t. #3 but would have full sky coverage.

The sensitivities for instruments #3-#5 are those given in table 3. The spectrographs would be a class of their own. In the near-infrared ( $1\mu m \leq \lambda \leq 2.5\mu m$ ), instrument #6 just starting to resolve the terrestrial absorption and emission lines would feature ultimate sensitivity. To give one example of a unique observing capability: scaling the performance of SOFI at the NTT correspondingly, one finds that the redshifted [OIII] and  $H_\alpha$  lines from the radio galaxy MRC 0406-244 (c.f. Moorwood et al. 1998) could be observed with  $0.5 \frac{km}{s}$  spectral resolution with either long-slit or integral field mode into spatial pixels of order 5-10mas, or 50-100 pc linear distance within that galaxy! The limiting magnitude for absorption line spectroscopy ( $10\sigma$  in  $1h$ ) at  $\lambda \approx 3.5\mu m$  could be expected to be 17.0 (and  $10.0^m$  at  $\lambda \approx 10\mu m$ )<sup>7</sup>. More general in the back-ground noise limited regime any object at the detection limit of the

<sup>7</sup>To put these sensitivities into context, for  $\lambda \approx 3.5\mu m$  this flux limit corresponds to  $\alpha - Sco$  at 2.0 Mpc.

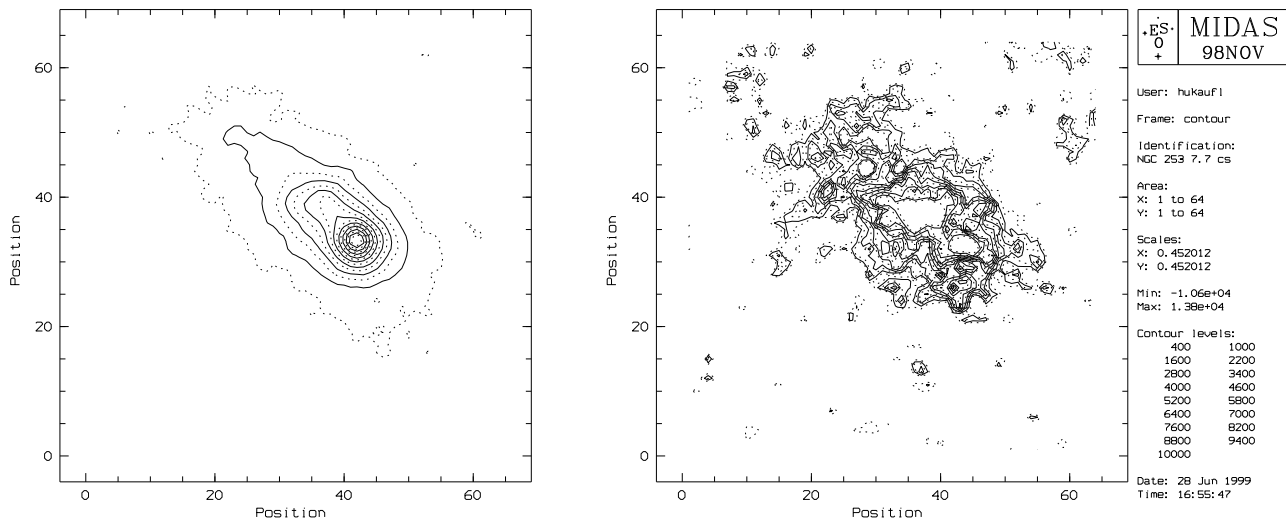


**Figure 1:** Images of the active galaxy NGC 253. The left image shows the galaxy at  $\lambda \approx 11.3\mu\text{m}$  while the right image shows the galaxy in the  $7.7\mu\text{m}$  transition of polyaromatic hydrocarbonates (continuum subtracted). The data have been taken with TIMMI (Käuffl et al. 1994) at ESO's 3.6m telescope on July 20, 1997. The scale is  $0.3\text{arcsec}/\text{pix}$ . While the left image was a matter of minutes, the  $\lambda \approx 7.7\mu\text{m}$  image is the concatenation of approximately 8 hours of observing (the terrestrial atmosphere is nearly opaque for this wavelength, see text). corresponding instrumentation at the VLT is accessible to these spectrographs.

## SOME SCIENTIFIC APPLICATIONS

### **Galactic Star Formation:**

The detailed processes required to assemble massive stars ( $M_{\star} \geq 8M_{\odot}$ ) are a matter of debate. The still accreting massive protostar is creating enough luminosity, hence radiative pressure, to balance gravitational accretion. As it is widely accepted that stars with  $M_{\star} \geq 8M_{\odot}$  exist, accretion free of interference from radiative pressure must be possible. Protostar accretion via a disk is one possibility. Until recently this has been the matter of theoretical conjecture. Accretion via a disk is one of the possibilities here. Stecklum et al. (work in progress)<sup>8</sup> recently found, observing with TIMMI (Käuffl et al., 1994) at  $\lambda \approx 10\mu\text{m}$ , a disk-like structure in the centre of the embedded ultracompact HII-region G339.88-1.26. This is most likely the first direct observational evidence of a disk around an O-star. Due to the relatively short lifetime of this phase this may be the only or closest such object observable. The object, however, is strongly obscured so that  $\lambda \approx 10\mu\text{m}$  is the shortest wavelength at which direct imaging is possible. While the formation and stability of a disk around the protostar is more or less straight forward to understand the real question remains: How can matter be accreted from the inner edge of the disk onto the star in spite of the strong radiative pressure? Only imaging with OWL and a spatial resolution of  $0.03\text{arcsec}$  (corresponding to a linear scale of several 100AU) can shed light on this particularly interesting problem which is of fundamental importance for the field of star formation. In combination with very high resolution moderate long-slit spectroscopy chemical composition, physical conditions and the Keplerian velocities of various regions of the disk could be determined.

### **Extragalactic Star Formation:**

In figure 1 (left) the centre of the active galaxy NGC 253 is shown in the mid-infrared dust continuum radiation. The exact nature of the dust and the heating mechanism, as well as the nature of the apparent unresolved peak in the image are unclear. The peak apparently is offset from the centre of the galaxy (e.g. Böker et al. 1998). The right part of figure 1 shows the same area with identical registration using a narrow-band filter, centered around the  $7.7\mu\text{m}$  transition associated with polyaromatic hydrocarbonates (PAH). This transition is believed to be produced by transient heating of macro-molecular associations by UV-photons. Therefore the radiation is the signature of carbon-bearing dust illuminated by a strong UV-radiation field. It is hence considered the signature of massive star

<sup>8</sup>See also ESO Press Release 08-98.

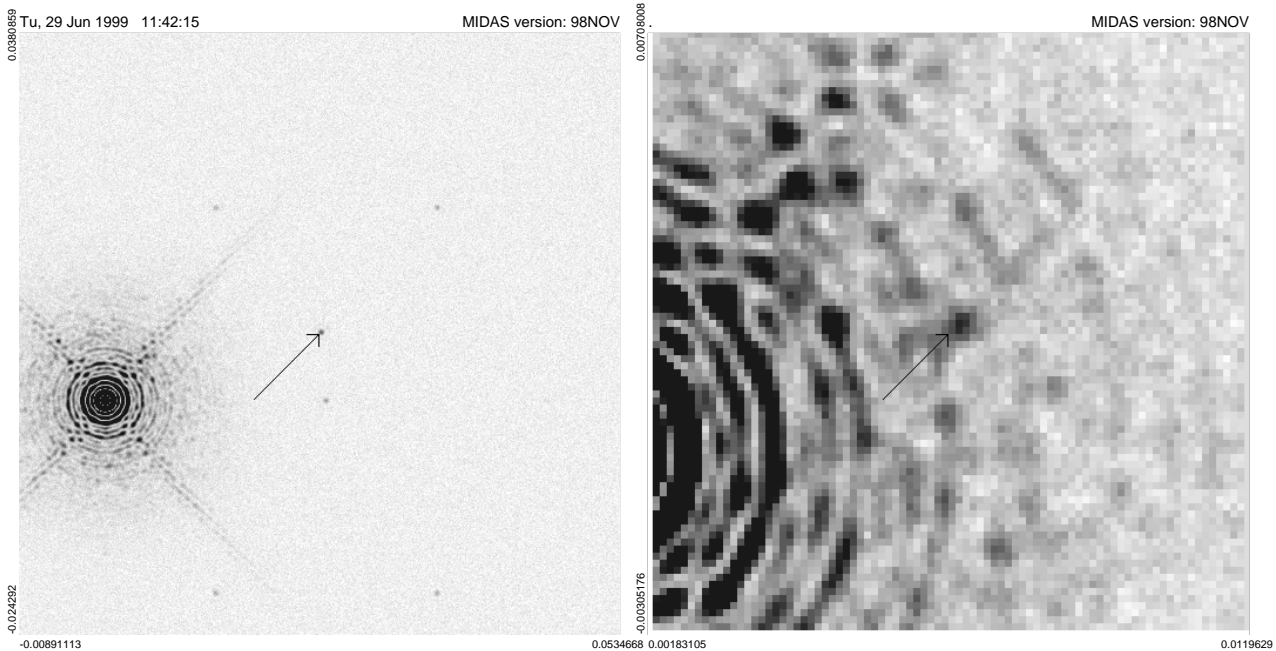


**Figure 2:** Simulated images of a Jupiter-like (left) and an Earth-like (right) planet around the G2 star  $\alpha_1 - Cen$  at a wavelength of  $18.5\mu m$ . At this distance the projected distances were chosen to be 2.15 and 0.68 arcsec, corresponding to a linear scale of 2.8 and 0.9 AU. For this image it was assumed, that the image of  $\alpha_1 - Cen$  could be cancelled by subtraction by a factor of 100. The pixel scale in both images is  $0.0111 \frac{arcsec}{pixel}$ . In the case of Jupiter a larger part of the image is shown, giving the overexposed diffraction pattern. The assumptions for this images are from a technical point of view neither particularly conservative nor optimistic (see text).

formation. As can be seen in figure 1, right, one sees a fairly symmetric zone of star formation, offset from the continuum peak in the direction of what is believed to be the centre of the galaxy, whereby the point source has disappeared. This nicely confirms the theory of a massive star-burst around the active nucleus of this galaxy. These data invite very exciting follow-up work with OWL. As NGC 253 is very close ( $\approx 3 Mpc$ , Madore & Friedman, 1992) follow-up with OWL would allow to study the morphology of star burst with  $0.4pc$  spatial resolution while allowing at the same time to investigate the nature of the up-to-now enigmatic continuum point source near the nucleus.

Particularly interesting, however, is that the observations presented in figure 1 were extremely difficult (see caption). With only a very small red-shift ( $z \geq 0.04$ ) the transition is shifted into the clear part of the  $10\mu m$  window. Technically, it could then be observed from the ground up to ( $z \approx 0.7$ ). Taking a recent compilation of ISO-spectra (c.f. Genzel et al. 1998) it can be expected that a great number of galaxies could be detected with OWL in this transition. Most IRAS ultra-luminous galaxies are exceeding the limiting flux of OWL at  $\lambda \approx 10\mu m$  by orders of magnitude, i.e. the spatially resolved study of starbursts in the obscured nuclei of many galaxies becomes feasible up to redshifts of 0.7!

### Extrasolar Planets:

Earth-like and Jupiter-like planets can be detected with OWL at  $\lambda \approx 10 - 20\mu m$  easily up to a distance of  $10 pc$ . The problem, however, is that the star will be of order  $10^5$  to  $10^6$  times brighter. To analyze the feasibility of a planet search by direct imaging an assumption of the point spread function of OWL had to be made. For that we used the design as presented earlier (Gilmozzi et al. 1998) and a scaled-up version of the spider geometry of ESO's Very Large Telescope. The entrance pupil, including the segmentation pattern, was then constructed and, together with a random phase screen approximating various seeing conditions (or imperfections of the AO system), numerically Fourier-transformed to arrive at a reasonable approximation of the OWL psf (as shown in fig. 2). It should be noted, that numerical restrictions allow only  $8k \times 8k$  arrays at this point for the maximum format for the entrance pupil approximation; this corresponds to a linear scale of  $0.10 - 0.20m$  per pixel in the OWL primary mirror plane. Thus the diffraction effects are grossly exaggerated. The psf upon which fig. 2 is based is the monochromatic case. A polychromatic calculation, which has not been done yet, will *dilute* the diffraction pattern. In the same

sense the rotation of the entrance pupil pattern w.r.t. the sky, OWL being an alt-az-mounted telescope, will lead to further smearing out of the diffraction pattern, thus improving the detectability. In this sense the results shown in fig. 2 are a worst case estimate and we have not yet resorted to other techniques such as apodization etc. It needs emphasizing, however, that also the zodiacal light around the star, which has been neglected here, will constitute another source of background, against which at least the detection of an Earth-like planet may be more challenging. Still also in this case the point spread function of a filled aperture 100m class telescope is by far the best means to enhance contrast between planets and the spatially extended zodiacal emission. In conclusion, however, OWL with a  $20\mu\text{m}$ -camera will allow the detection of Earth-like planets around neighbouring stars (c.f. fig. 2). Provided a suitable very-high resolution near infrared spectrograph becomes available at the OWL, then a simple spectroscopic confirmation of oxygen on such a planet is feasible by searching for atmospheric OH-emission lines (instrument #6 above is just barely resolving these lines which have intrinsic widths of order of  $1\frac{\text{km}}{\text{s}}$  and thus provides ultimate sensitivity/contrast for detection). Unfortunately, however, at  $\lambda \approx 1.7\mu\text{m}$  the contrast has been estimated, based on the terrestrial OH-airglow at twilight, to be again of order of  $10^5$  to  $10^6$ , thus the combination of very high spectral resolution and very high spatial resolution in long-slit mode are essential.

## OUTLOOK AND FUTURE WORK

In summary an infrared instrumentation complement of OWL appears highly desirable and highly competitive. Of particular value are instruments designed around a dedicated integrated adaptive optics system (DAVID). In the range  $1\mu\text{m} \leq \lambda \leq 2.5\mu\text{m}$  instruments based on natural guide star AO systems in combination with OWL will not feature full sky coverage, but absolutely unique sensitivity, spatial resolution and spectral resolving power. In the range  $3\mu\text{m} \leq \lambda \leq \approx 25\mu\text{m}$  instruments based on natural guide star AO systems in combination with OWL have practically full sky coverage and will feature - compared to a 8m space telescope - not necessarily ultimate sensitivity but absolutely unique spatial and spectral resolving power. Moreover, for survey work, these instruments can operate in a hitch-hiker mode.

From the technical point of view, all items required (detectors, optics, mechanics) appear to be in the extrapolation range of today's instruments for 8m class telescopes. The biggest challenges in this context appear to be the size of the filters and the size (hence weight and flexure) of the instrument cold structure.

A detailed analysis as to the scientific merits of conventional instruments not using adaptive optics (GOLIATHs) is still required.

## REFERENCES:

- Böker, T., Krabbe, A., & Storey, J.W.V., 1998, **APJ** **498**, L115
- Finger, G. et al. 1998, Proc. SPIE **3354**, p. 87-98, *Infrared Astronomical Instrumentation*, Albert M. Fowler *Editor*
- Genzel, R., Lutz, D., Sturm, E., et al., 1998, **APJ** **498**, 579
- Gilmozzi, R., Delabre, B., Dierickx, P., HUBIN, N., et al. Proc. SPIE Vol. 3352, p. 778-791, *Advanced Technology Optical/IR Telescopes VI*, Larry M. Stepp; *Editor*
- Käuff, H.-U., Jouan, R., Lagage, P.O., Masse, P., Mestreau, P., Tarrus, A., 1994, *Infrared Phys. Technol.* **35**, 203
- Käuff, H.U., Kühl K., & Vogel S., Proc SPIE Vol. 3354, p. 151-158 *Infrared Astronomical Instrumentation*, Albert M. Fowler; *Editor*
- Kozlowski, L.J. et al., 1996, Proc. SPIE **2746**, p. 93-100
- Madore, B.F. & Freedman, W.L., 1992, **PASP** **104**, 362
- Merkle F., 1988, Proc. ESO conference on *Scientific Importance of High Angular Resolution at IR and Optical Wavelengths*, ESO, Garching, 639
- Moorwood, A.F.M. et al. 1998 *The Messenger* **91** 1
- Moorwood, A.F.M. et al. 1999 *The Messenger* **95** 1
- Reimann, H.-G., Weinert, U., & Wagner, S., 1998 Proc. SPIE **3354**, p. 865-876, *Infrared Astronomical Instrumentation*, Albert M. Fowler *Editor*